New Phytologist

Research

Rapid report

Disruption of stomatal lineage signaling or transcriptional regulators has differential effects on mesophyll development, but maintains coordination of gas exchange

Author for correspondence:
Dominique C. Bergmann
Tel: +1 650 736 0983
Email: dbergmann@stanford.edu

Received: *6 June 2017*
Accepted: *14 July 2017*

Graham J. Dow[1], Joseph A. Berry[2] and Dominique C. Bergmann[3,4]

[1]Department of Biology, Boston University, Boston, MA 02215, USA; [2]Department of Global Ecology, Carnegie Institution for Science, Stanford, CA 94305, USA; [3]Department of Biology, Stanford University, Stanford, CA 94305, USA; [4]HHMI, Stanford University, Stanford, CA 94305, USA

New Phytologist (2017) **216:** 69–75
doi: 10.1111/nph.14746

Key words: *Arabidopsis thaliana*, gas-exchange capacity (g_{smax}), leaf photosynthetic potential (V_{cmax}), mesophyll development, stomatal development, water-use efficiency.

Summary

- Stomata are simultaneously tasked with permitting the uptake of carbon dioxide for photosynthesis while limiting water loss from the plant. This process is mainly regulated by guard cell control of the stomatal aperture, but recent advancements have highlighted the importance of several genes that control stomatal development.
- Using targeted genetic manipulations of the stomatal lineage and a combination of gas exchange and microscopy techniques, we show that changes in stomatal development of the epidermal layer lead to coupled changes in the underlying mesophyll tissues. This coordinated response tends to match leaf photosynthetic potential (V_{cmax}) with gas-exchange capacity (g_{smax}), and hence the uptake of carbon dioxide for water lost.
- We found that different genetic regulators systematically altered tissue coordination in separate ways: the transcription factor SPEECHLESS (SPCH) primarily affected leaf size and thickness, whereas peptides in the EPIDERMAL PATTERNING FACTOR (EPF) family altered cell density in the mesophyll. It was also determined that interlayer coordination required the cell-surface receptor TOO MANY MOUTHS (TMM).
- These results demonstrate that stomata-specific regulators can alter mesophyll properties, which provides insight into how molecular pathways can organize leaf tissues to coordinate gas exchange and suggests new strategies for improving plant water-use efficiency.

Introduction

Recent attention has turned to the contributions of stomatal development in optimizing plant–environment relationships and controlling physiological performance (Chater *et al.*, 2014; Dow & Bergmann, 2014; Lawson & Blatt, 2014). Enabling this focus is the availability of genetic resources to modify stomatal numbers and their distribution, or pattern, on the leaf surface (Lau & Bergmann, 2012; Pillitteri & Torii, 2012). Several groups have analyzed mutants or transgenic lines that specifically altered stomatal lineage transcription factors or signaling components with traditional physiological and environmental tools (Doheny-Adams *et al.*, 2012; Tanaka *et al.*, 2013; Dow *et al.*, 2014b; Franks *et al.*, 2015). Gas-exchange experiments in *Arabidopsis thaliana* identified a connection between g_{smax}, the anatomical maximum rate of stomatal conductance as defined by stomatal size and density, and photosynthetic rate (Dow *et al.*, 2014a,b). When g_{smax} was substituted for net carbon assimilation (A) in the Ball–Berry equation (Ball *et al.*, 1987), this derived model was capable of predicting operational stomatal conductance. The ability to substitute g_{smax} for A hinted at an underlying link between stomatal development and the photosynthetic potential of the leaf**.** Here, we investigate the impact of genetic manipulations in the stomatal lineage on the developmental organization and physiological capacity of the mesophyll tissue.

Materials and Methods

Plant materials and growth conditions

All genotypes tested were in the Columbia (Col-0) ecotype of *Arabidopsis thaliana* (L.) Heynh. and Col-0 was used as the control in all experiments. The following previously described genotypes were used: *epf1* and *tmm;epf1* (Hara *et al.*, 2007); *epf2*, *epf1;epf2*, and *tmm;epf2* (Hunt & Gray, 2009); $35S_{pro}$:EPF1 and $35S_{pro}$:EPF2 (Hara *et al.*, 2009); $SPCH_{pro}$:SPCH-YFP and $SPCH_{pro}$:SPCH 2-4A-YFP (Lampard *et al.*, 2008); SPCH SILENCE (Dow *et al.*, 2014b); *basl* (Dong *et al.*, 2009); *tmm-1* (Nadeau & Sack, 2002); *erecta-105* (Torii *et al.*, 1996); *tmm;erecta* (Shpak *et al.*, 2005); $35S_{pro}$:EPFL9OX and $35S_{pro}$:EPFL9RNAi, referenced in this manuscript as STOMAGEN OX and STOMAGEN RNAi, respectively (Hunt *et al.*, 2010). Seeds were surface-sterilized and stratified at 4°C for 3–5 d in 0.15% agarose solution and then sown directly into Pro-Mix HP soil (Premier Horticulture; Quakerstown, PA, USA) and supplemented with Scott's Osmocote Classic 14-14-14 fertilizer (Scotts-Sierra, Marysville, OH, USA). At 10–14 d, seedlings were thinned so only one seedling per container remained. Plants were grown to maturity in growth chambers where the conditions were as follows: 16 : 8 h, 22 : 20°C, day : night cycle, *c.* 100 μmol photon m^{-2} s^{-1}, unless otherwise noted.

Calculating V_{cmax}

Gas-exchange measurements were taken on the largest and most accessible mature rosette leaf of stomatal development mutants and control plants at 5–7 wk post germination using a LI-6400 Portable Photosynthesis System with the 6400-02B LED Light Source (Li-Cor Biosciences Inc., Lincoln, NE, USA). Gas-exchange measurements were performed as described in Dow *et al.* (2014a,b) and the steady-state response of net carbon assimilation (A) to intercellular CO_2 concentration (c_i) was obtained from stepping ambient CO_2 at 100 ppm to 350, 500, 750 and 1000 ppm. V_{cmax} for each leaf was calculated by fitting individual A–c_i response curves to a biochemical model of C3 photosynthesis (Farquhar *et al.*, 1980) using an IDL GUI computational tool developed by Bob Haxo and Joe Berry.

Calculating g_{smax}

Rosette leaves used in gas-exchange experiments were prepared for stomatal phenotype analysis and quantified as described in Dow *et al.* (2014a,b). Maximum stomatal conductance to water vapor as defined by stomatal anatomy (g_{smax}, mol H_2O m^{-2} s^{-1}) was estimated for each leaf using a double end-correction version of the equation by Franks & Farquhar (2001):

$$g_{s\,max} = \frac{d\,Da_{max}}{v\left[1 + \frac{\pi}{2}\sqrt{\frac{a_{max}}{\pi}}\right]} \qquad \text{Eqn 1}$$

where d is the diffusivity of water in air (m^2 s^{-1}, at 22°C), v is the molar volume of air (m^3 mol^{-1}, at 22°C), π is the mathematical constant, approximated to 3.142, D is stomatal density (mm^{-2}), l is pore depth (μm), which was equal to guard cell width at the center of the stoma, and a_{max} is the mean maximum stomatal pore area (μm^2), which was defined as an ellipse with major axis equal to pore length and minor axis equal to half pore length. g_{smax} for each leaf was calculated as the sum of g_{smax} abaxial (g_{ab}) and g_{smax} adaxial (g_{ad}) using empirical values of D, l and a_{max} for stomata on each side of the leaf ($g_{smax} = g_{ab} + g_{ad}$). D was determined independently for each leaf, while values of l and a_{max} were genotype averages.

Three-dimensional confocal imaging of leaf morphology

Imaging of the epidermis and internal leaf structures was performed using a Leica SP5 confocal microscope with the protocol developed by Wuyts *et al.* (2010). Preparation of samples was performed as described, except for the following modifications at the end of the protocol: leaves were stained by propidium iodide overnight in water and then mounted in Hoyer's solution directly on a microscope slide. Leaves were thoroughly immersed in Hoyer's solution to prevent desiccation and were left exposed to air until the leaves were transparent, at which point a cover slip was applied and imaging was performed within 48 h. Only the sixth rosette leaf was used for analysis and four areas in the midleaf region, between the midvein and leaf edge, were imaged per leaf. At each location, a z-stack of images (x–z plane; see later Fig. 2a) at intervals of 2 μm was taken to span all leaf tissues, from adaxial to abaxial epidermis. Cell densities of the adaxial epidermis and palisade mesophyll were determined by hand using the Cell Counter in FIJI (NIH; www.fiji.sc/Fiji). A transvere cross-section of the entire leaf (x–z plane, see later Fig. 2a) was produced using the Dynamic Reslice function in FIJI on a complete z-stack. Leaf thickness was determined by measuring the distance betweeen the top of the adaxial epidermis and the bottom of the abaxial epidermis at three points across the image. Measurement points were visually chosen at the maximum thickness in an area, and the average of all measurements was used to define leaf thickness. Determination of leaf thickness on dehydrated samples probably underestimated the true thickness, but this error should be consistent across all samples. Leaf area was determined by outlining in pen the leaf mounted on a microscope slide, imaging the slide with a Hewlett-Packard printer-scanner, and calculating the area within the leaf outline using FIJI's Tracing Tool.

Carbon isotope analysis

Arabidopsis thaliana seeds from a subset of genotypes were used to determine ^{13}C : ^{12}C isotope ratios. Although of the same genotype and lineage, seeds used in this analysis were not from the identical plants used in gas-exchange measurements or confocal analysis of stomatal traits. Genotypes were simultaneously grown to maturity in one growth chamber, under conditions as follows: 16 : 8 h, 22 : 20°C, day : night cycle, *c.* 100 mmol photon m^{-2} s^{-1}, *c.* 65% relative humidity, soil water content maintained at 70% field capacity, and ambient [CO_2] of *c.* 425 ppm. A 2.000 mg quantity of seed was weighed and packaged in a foil ball, six replicates were performed per genotype. Samples were combusted in a Carlo Erba Combustion Elemental Analyzer (Thermo Scientific Inc.,

Watham, MA, USA) and the resultant gas was analyzed in a Delta V Advantage Mass Spectrometer (Thermo Scientific Inc.). The carbon isotope ratio of seed tissue ($\delta^{13}C$) in units per mil (‰) was calculated as:

$$\delta^{13}C(‰) = (R_{sample}/R_{standard} - 1) \times 1000 \quad \text{Eqn 2}$$

where R_{sample} and $R_{standard}$ are the $^{13}C : {}^{12}C$ ratios of seeds and the V-PDB standard, respectively.

Statistical analysis

All statistical analysis was performed using R (http://www.r-project.org/). Linear regression models were used to determine variance (adjusted R^2) and the statistical significance of covariation between parameters ($P < 0.05$). Comparison of regression models was performed by ANCOVA to determine significance between regression slopes (effect of genotype on dependent variable) or y-intercepts (quantitative differences between genotypes). Comparison of mean values between Col-0 and all other genotypes was performed by Wilcoxon signed-rank t-tests for unpaired, nonparametric samples ($P < 0.05$).

Results and Discussion

To explore the linkages between the stomatal lineage and mesophyll tissue, we analyzed carbon assimilation–intercellular CO_2 (A–c_i) response curves to determine V_{cmax}, the maximum rate of carboxylation as limited by the ribulose 1,5-bisphosphate carboxylase-oxygenase enzyme (Rubisco). We sampled from gas-exchange experiments of five stomatal development mutant lines and Col-0 grown at three different fluence rates (50, 100 and 200 μmol photons m^{-2} s^{-1}) as presented in Dow *et al.* (2014a,b). Indeed, there was a significant and positive relationship between V_{cmax} and g_{smax} across all lines (Fig. 1; $R^2 = 0.934$, $P < 0.001$, n individuals = 46). While the response in V_{cmax} across Col-0 light treatments was expected, we anticipated that changes in g_{smax} derived from genetic manipulations that target the epidermis would segregate independently from V_{cmax}. However, our results indicate the opposite: g_{smax} was strongly correlated with V_{cmax} across a wide physiological spectrum.

V_{cmax} is directly related to the amount of Rubsico in the leaf (von Caemmerer & Farquhar, 1981). Our mutant lines specifically targeted the stomatal lineage, yet altering epidermal cell properties appeared to change the quantity of Rubisco in the mesophyll. If the ratio of $g_{smax} : V_{cmax}$ remained stable across genotypes, one might predict that intrinsic water-use efficiency (W_g) should remain constant as well. As an indicator of W_g we measured carbon isotope composition (Seibt *et al.*, 2008), $\delta^{13}C$, among the mutants and Col-0 (for comparative purposes, a more negative $\delta^{13}C$ indicates a lower W_g). Carbon isotope measurements have previously been used to assess genetic variation in W_g because the fractionation process integrates both the diffusion and carboxylation limitations of CO_2 uptake (Masle *et al.*, 2005). Genetic controls over W_g could result from variation in stomatal properties, from modifications to the mesophyll, or from changes in both

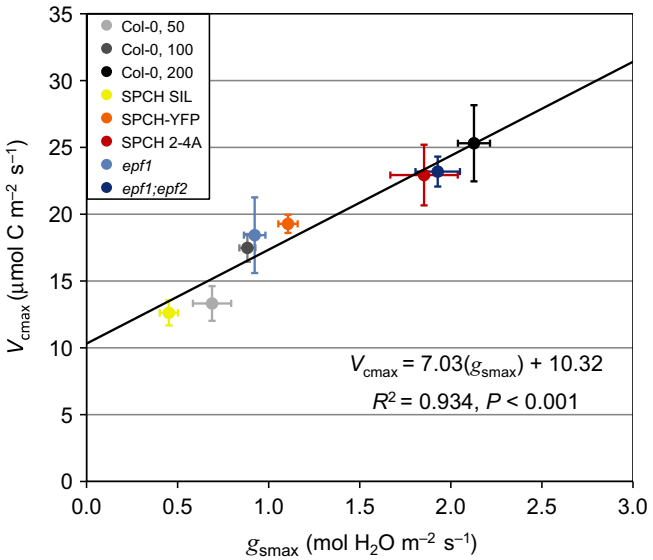

Fig. 1 Changes in gas-exchange capacity (g_{smax}) driven by genetic regulators of stomatal development are correlated with changes in leaf photosynthetic potential (V_{cmax}). *Arabidopsis thaliana* Col-0 plants were grown at three different fluence rates (50, 100, and 200 μmol photons m^{-2} s^{-1}), while all other genotypes were grown at 100 μmol photons m^{-2} s^{-1}. All individuals were grouped by genotype or light treatment and the mean values of each group were used for the regression model, which showed a positive correlation between g_{smax} (the maximum rate of stomatal conductance as defined by stomatal size and density) and V_{cmax} (the maximum rate of Rubisco carboxylation) ($R^2 = 0.934$, $P < 0.001$, no. of individuals = 46). Error bars are ±SEM.

tissues. In our study, we found no significant differences in $\delta^{13}C$ among mutants or transgenics despite large differences in stomatal properties (Supporting Information Table S1). This isotopic evidence further confirmed our hypothesis of interlayer developmental coordination.

These initial findings indicated that targeted manipulations of the stomatal lineage in the epidermis were leading to concomitant changes in the underlying mesophyll tissues. Three-dimensional confocal microscopy techniques (modified from Wuyts *et al.*, 2010) allowed us to visualize the epidermis and adjacent internal structures of the leaf and therefore test this directly (Fig. 2a). We first imaged Col-0 leaves grown under standard or high-light conditions and focused on the relationship between the adaxial epidermis and the palisade mesophyll layer, where the majority of photosynthesis occurs (Fig. 2b–m). Plants grown in high light had increased stomatal density (Fig. 2b,e), increased palisade mesophyll density (Fig. 2f,i), and increased leaf thickness (Fig. 2j,m) relative to standard conditions, consistent with classical observations of 'sun' and 'shade' leaves across plant taxa (Nobel *et al.*, 1975; Terashima *et al.*, 2011). These structural changes enhance CO_2 transfer across the epidermis and increase the internal mesophyll surface area for CO_2 diffusion into cells, thereby enhancing photosynthetic capacity.

We then characterized interlayer coordination in mutant lines with increased stomatal production: one line expressed a hyperactive form of the SPCH transcription factor under its native promoter (active in the epidermis, SPCHp:SPCH 2-4A) and the

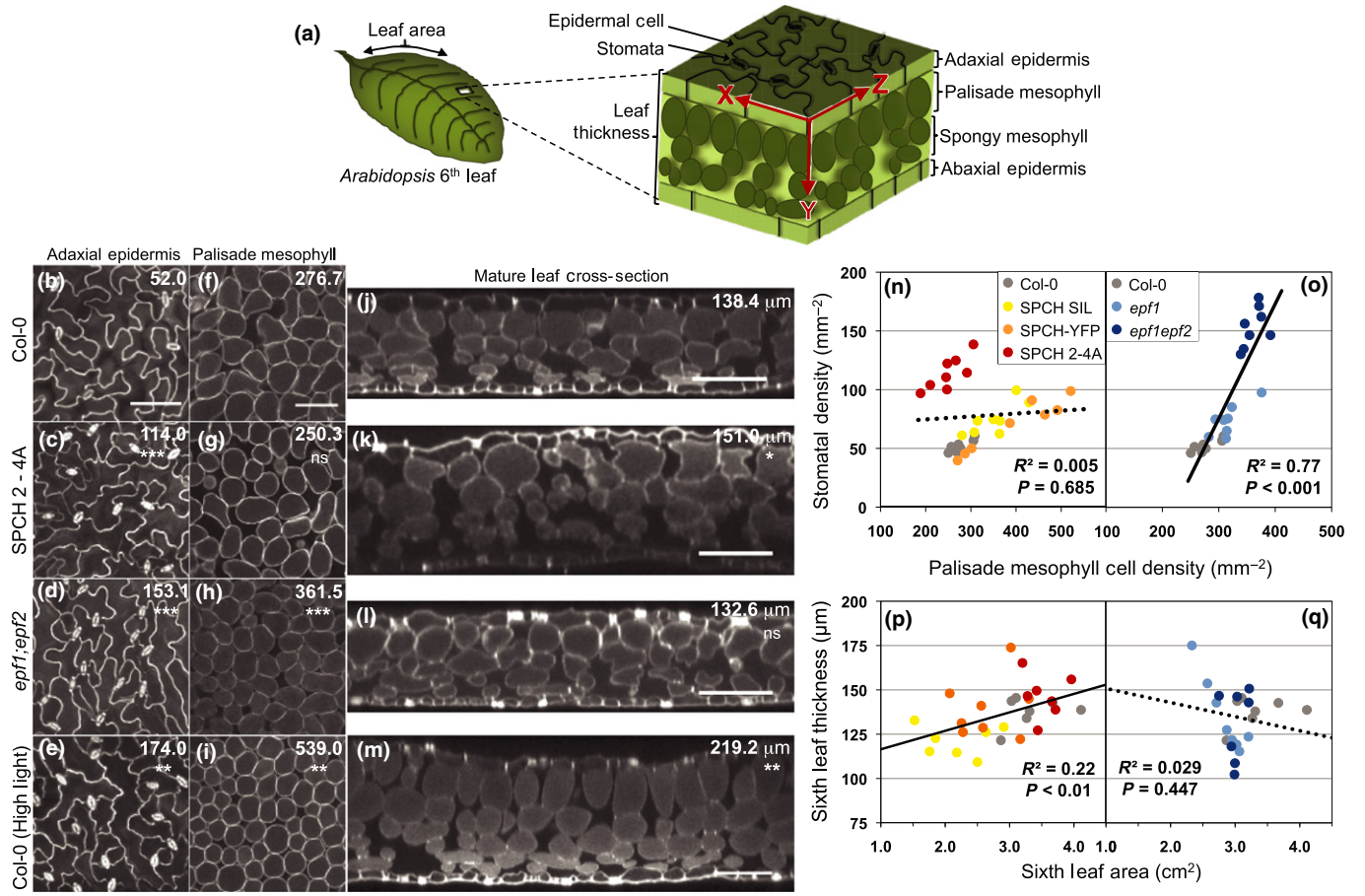

Fig. 2 High-resolution three-dimensional imaging of leaf morphology reveals two separate classes of mesophyll alterations in stomatal development mutants. Images of *Arabidopsis thaliana* (b–e) depict an *x*–*z* planar view of the adaxial epidermis (see panel (a) for spatial relationships); all images of the epidermis are at the same magnification. (f–i) An *x*–*z* planar view of the palisade mesophyll cell layer; all images of the mesophyll are at the same magnification. (j–m) An *x*–*y* planar cross-section of the mature leaf. Bars, 100 µm. The genotypes for each row of images are defined in the left margin and values in the top right corner of each image are genotype averages of stomata density (b–e), palisade cell density (f–i), or leaf thickness (j–m). Notation below the numbers indicates significant difference from Col-0: ns, $P > 0.05$; *, $P < 0.05$; **, $P < 0.01$; ***, $P < 0.001$. All images were taken from the sixth rosette leaf ($n = 8$ for Col-0, SPCH 2-4A, and *epf1;epf2*; $n = 4$ for Col-0 grown under high light). All SPEECHLESS (SPCH) and *epidermal patterning factor* (*epf*) lines were then grouped separately for regression analysis to determine relationships between adaxial stomatal density and palisade mesophyll cell density (n–o) and leaf thickness with leaf size (p–q). The regression analysis for each group includes the Col-0 control plants. SPCH plants showed no significant relationship between cell type densities (n) ($R^2 = 0.005$, $P = 0.685$, $n = 32$) as indicated by the dotted line, but leaf thickness increased as a function of leaf area (p) ($R^2 = 0.22$, $P < 0.01$, $n = 29$), as indicated by the unbroken line. *epf* plants showed a positive relationship between cell type densities (o) ($R^2 = 0.77$, $P < 0.001$, $n = 24$), but leaf thickness and leaf area were not correlated (q) ($R^2 = 0.029$, $P = 0.447$, $n = 22$).

second was a mutant for the stomatal lineage expressed EPF peptide ligands (*epf1;epf2*). Both manipulations changed mesophyll structure (Fig. 2g,k, and 2h,l, respectively), but, unexpectedly, they changed in distinct ways. SPCH 2-4A plants primarily displayed an increase in leaf thickness (Fig. 2j–l), while *epf1;epf2* plants increased palisade mesophyll cell density (Fig. 2f–h). Essentially, the changes in mesophyll phenotypes observed when wild-type plants were subjected to high light were divided into discrete subresponses in these two genotypes. We tested additional related genotypes (SPCH-YFP, SPCH SIL, and *epf1*) to explore whether these coordinate changes were specific to the respective functional classes (Fig. 2n–q). *epf* mutants had a strong positive correlation between cell type densities ($n = 24$, $R^2 = 0.77$, $P < 0.001$; Fig. 2o), while multiple SPCH lines demonstrated no consistent pattern between stomatal and palisade mesophyll cell density ($n = 32$, $R^2 = 0.005$, $P = 0.685$; Fig. 2n). Conversely, SPCH mutants had significant increases in leaf thickness, as well as overall leaf area ($n = 32$, $R^2 = 0.22$, $P < 0.01$; Fig. 2p) in direct correlation with increasing g_{smax} (SPCH SIL < SPCH-YFP < SPCH 2-4A), while *epf* mutants had no such differences in thickness or area ($n = 24$, $R^2 = 0.029$, $P = 0.447$; Fig. 2q).

The distinct effect of functional gene classes on mesophyll architecture implied that multiple mechanisms are responsible for coordination between g_{smax} and V_{cmax}. Manipulating SPCH activity changed the extent of proliferation of the stomatal lineage, which increased production of nonstomatal epidermal cells that ultimately regulate leaf area (Lampard *et al.*, 2008; Gonzalez *et al.*, 2012). We found that leaf area was positively correlated with leaf thickness, which provided for increased cell density in three-dimensional space and resultant increases in photosynthetic capacity (Terashima *et al.*, 2006). This relationship was specific to manipulation of SPCH activity rather than manipulation of the

stomatal lineage in general, as EPF mutants revealed no change in leaf area. In comparison, the change in mesophyll architecture for EPF mutants appears to be a more local event: changing the density of palisade mesophyll cells immediately below the adaxial epidermis rather than having a global effect on leaf area or thickness. Changes in mesophyll cell density were correlated with photosynthetic capacity presumably because of changes in total cell surface area, but the shape of the cells and how they pack together may also have affected surface area. Whether the local density relationship is maintained at the interface between the abaxial epidermis and the spongy mesophyll tissue was harder to determine because of the irregular spatial organization of the spongy cells and requires further investigation. To our knowledge, these results provide the first evidence that genetic changes in the stomatal lineage are linked with developmental responses in mesophyll structure. This form of interlayer communication plays a critical role in plant physiology because it appears to optimize gas exchange by matching the supply and demand for CO_2. Our results also indicate that growth environment plays a significant role in this developmental process. For example, when wild-type plants and EPF mutants are grown under full sunlight, differences in V_{cmax} are insignificant while changes in g_{smax} driven by EPF activity remain (Franks *et al.*, 2015). Growth under high- or low-intensity light could also help to explain the observed differences in W_g as measured by carbon isotope composition across these different studies (Franks *et al.*, 2015).

Despite these environmental influences, this type of developmental linkage provides a blueprint for harnessing stomatal development to alter biochemical capacity in the mesophyll. One stomatal regulator that can strongly influence W_g is ERECTA (Masle *et al.*, 2005), a receptor-like kinase that mediates EPF signaling (Lee *et al.*, 2012, 2015). ERECTA was demonstrated to influence both the proliferation of stomata in the epidermis and mesophyll cell development (Masle *et al.*, 2005). In light of our work, this dual role appears to be a critical link for improving W_g. To pursue a potential mechanism, we sampled mutants of the cell surface receptor genes, *ERECTA* and *TMM*, and additional lines of the *EPF* family, including *STOMAGEN*, an antagonist of EPF1 and EPF2 activity that travels from the mesophyll to the epidermis (Sugano *et al.*, 2009; Hunt *et al.*, 2010). Loss of function or overexpression of STOMAGEN was consistent with similar manipulations of EPF1 and EPF2, in that stomatal density and palisade cell density remained positively correlated ($n = 35$, $R^2 = 0.54$, $P < 0.001$; Fig. 3a). While each of the EPF family members affected the overall 'set point' of epidermal and mesophyll cell numbers, all lines remained consistent with respect to interlayer coordination, thus ruling them out as the required signal. By contrast, *erecta* and *tmm* had quantifiably opposite effects on the density of stomata and palisade mesophyll cells. *erecta* increased adaxial stomatal density and trended toward decreased palisade mesophyll density relative to Col-0 ($P < 0.001$ and $P = 0.128$, respectively; Fig. 3b and Table S2). *tmm* had the reverse effect – a decrease in adaxial stomata but an increase in palisade mesophyll density ($P < 0.001$ and $P < 0.01$, respectively; Fig. 3b and Table S2). Essentially, mutations in these coreceptors broke the developmental coordination between epidermal and mesophyll tissues.

This conclusion was further corroborated by carbon isotope analysis, as *tmm* had a −2.1‰ difference relative to Col-0 ($\delta^{13}C$ of −31.8‰ and −33.9‰, respectively, $P < 0.01$), which implies an improvement in W_g. *ERECTA* mutants exhibited the opposite trend, consistent with the published difference of +1.1‰ (Masle *et al.*, 2005). The change in $\delta^{13}C$ for *tmm* was not the result of changes in stomatal conductance owing to stomatal clustering, as a control line for clustering (*basl*; characterized in Table S2 and Dow *et al.*, 2014a,b) was no different from Col-0 (−33.9‰ and

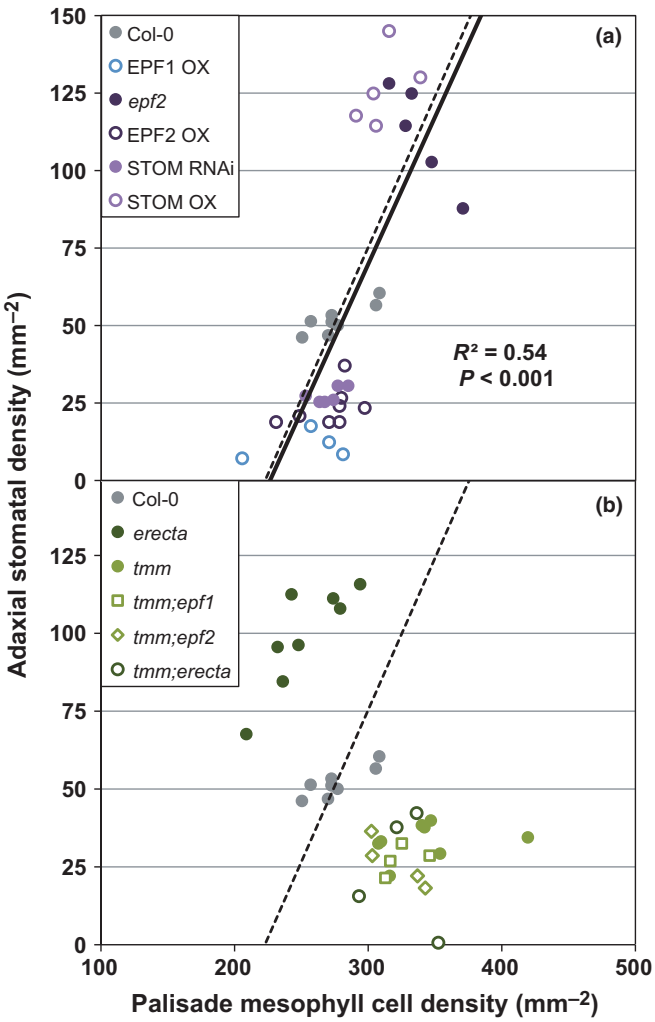

Fig. 3 Cell surface receptors, but not ligands, involved in stomatal development can disrupt the coordination between epidermal and mesophyll cell densities. In panel (a), manipulation of various EPIDERMAL PATTERNING FACTORS (EPFs) in *Arabidopsis thaliana* mirrors the epidermal–mesophyll relationship shown in Fig. 2(o) (solid line, $R^2 = 0.54$, $P < 0.001$, $n = 35$). The dashed lines in (a, b) refer to the regression model from Fig. 2(o); comparison of regression models was not significantly different in (a) (ANCOVA, $P = 0.896$). In (b), loss of cell surface receptors TOO MANY MOUTHS (TMM) and ERECTA altered the relationship between adaxial stomatal density and palisade mesophyll cell density in opposite ways. *erecta* plants increased adaxial stomata but decreased mesophyll cell density, while *tmm* decreased adaxial stomata and increased mesophyll cell density (see also Supporting Information Table S2). *tmm* was epistatic in all double mutant combinations tested (see also Table S3).

−33.9‰, respectively, $P = 0.675$). These isotopic results imply that *TMM* can negatively regulate W_g, which directly antagonizes the previously identified role of *ERECTA* (Masle *et al.*, 2005). While the *erecta* mutant has multiple effects on plant architecture resulting from widespread expression patterns, *ERECTA*'s genetic relationship with *TMM* and their opposing effects on $\delta^{13}C$ indicate that coordination of leaf epidermal and mesophyll development is instrumental in the determination of W_g. In addition, the epidermal-specific TMM appears to be the critical mediator of the interlayer signaling process: loss of *TMM* was epistatic to loss of the *EPF* ligands, and, most interestingly, it was epistatic to loss of its coreceptor *ERECTA* (Fig. 3b; Table S3). Both synergistic and antagonistic relationships between *ERECTA* and *TMM* have been described for developmental responses within the stomatal lineage (Shpak *et al.*, 2005; Qi *et al.*, 2017). How these coreceptors manifest opposite effects on interlayer coordination remains unknown: the TMM-ERECTA receptor complex may receive and propagate a direct signal to coordinate interlayer development or it might act through some secondary and more indirect mechanism. Regardless, the capacity to disrupt interlayer coordination indicates that this process is genetically defined over developmental timescales and relies upon signaling in the epidermis. This distinguishes interlayer coordination from being a strictly homeostatic mechanism responding to changes in stomatal conductance, photosynthesis, leaf water status, sugar content, or another indicator of leaf physiology.

Our study reinforces the importance of developmental coordination between leaf tissues and identifies a multifaceted process in leaves that appears dependent on both local communication and tissue-wide responses to align gas-exchange potential with photosynthetic capacity. While the full mechanism driving coordination remains unknown, elements of the developmental process can be separated into at least two subcategories: cellular density and leaf thickness. The former process, observed here as parallel changes in palisade mesophyll density and adaxial stomatal density, requires TMM signaling, potentially acting in opposition to its coreceptor ERECTA. Understanding how TMM and ERECTA drive changes in leaf development across tissue layers is a potentially rewarding avenue for improving plant water-use efficiency. Independently altering the epidermal or mesophyll developmental process, or driving opposing responses, may reduce transpiration without compromising photosynthesis or plant growth. This approach also highlights an important caveat for genetic engineering of agricultural or bioenergy feedstocks: our efforts must consider the compensatory changes that are induced when manipulating plant anatomy and function. With respect to water-use efficiency, the developmental linkage between g_{smax} and V_{cmax} may be a valuable tool for measuring noncompensatory improvements in plant productivity and responses to key environmental parameters, such as increasing atmospheric CO_2 (Leakey *et al.*, 2009; Lammertsma *et al.*, 2011).

Acknowledgements

This work was supported by a Stanford University Bio-X Interdisciplinary Fellowship to G.J.D. and by funding from the Gordon and Betty Moore Foundation awarded to D.C.B., who is an investigator of the Howard Hughes Medical Institute. We thank Larry Giles for performing the carbon isotope analysis. STOMAGEN lines used in this study were the kind gift of Dr Julie Gray (University of Sheffield).

Author contributions

G.J.D., J.A.B., and D.C.B. designed the project, interpreted the data, and wrote the manuscript; G.J.D. performed the experiments.

References

Ball J, Woodrow I, Berry J. 1987. A model predicting stomatal conductance and its contribution to the control of photosynthesis under different environmental conditions. In: Biggens J, ed. *Prog. Photosynthesis Res. Proc. Int. Congress 7th, Providence; 10–15 Aug 1986, vol 4*. Boston, MA, USA: Kluwer: 221–224.

von Caemmerer S, Farquhar GD. 1981. Some relationships between the biochemistry of photosynthesis and the gas exchange of leaves. *Planta* **153**: 376–387.

Chater CCC, Oliver J, Casson S, Gray JE. 2014. Putting the brakes on: abscisic acid as a central environmental regulator of stomatal development. *New Phytologist* **202**: 376–391.

Doheny-Adams T, Hunt L, Franks PJ, Beerling DJ, Gray JE. 2012. Genetic manipulation of stomatal density influences stomatal size, plant growth and tolerance to restricted water supply across a growth carbon dioxide gradient. *Philosophical Transactions of the Royal Society B: Biological Sciences* **367**: 547–555.

Dong J, MacAlister CA, Bergmann DC. 2009. BASL controls asymmetric cell division in *Arabidopsis*. *Cell* **137**: 1320–1330.

Dow GJ, Bergmann DC. 2014. Patterning and processes: how stomatal development defines physiological potential. *Current Opinion in Plant Biology* **21C**: 67–74.

Dow GJ, Bergmann DC, Berry JA. 2014a. An integrated model of stomatal development and leaf physiology. *New Phytologist* **201**: 1218–1226.

Dow GJ, Berry JA, Bergmann DC. 2014b. The physiological importance of developmental mechanisms that enforce proper stomatal spacing in *Arabidopsis thaliana*. *New Phytologist* **201**: 1205–1217.

Farquhar GD, von Caemmerer S, Berry JA. 1980. A biochemical model of photosynthetic CO_2 assimilation in leaves of C_3 species. *Planta* **149**: 78–90.

Franks PJ, Doheny-Adams TW, Britton-Harper ZJ, Gray JE. 2015. Increasing water-use efficiency directly through genetic manipulation of stomatal density. *New Phytologist* **201**: 188–195.

Franks PJ, Farquhar GD. 2001. The effect of exogenous abscisic acid on stomatal development, stomatal mechanics, and leaf gas exchange in *Tradescantia virginiana*. *Plant Physiology* **125**: 935–942.

Gonzalez N, Vanhaeren H, Inze D. 2012. Leaf size control: complex coordination of cell division and expansion. *Trends in Plant Science* **17**: 332–340.

Hara K, Kajita R, Torii KU, Bergmann DC, Kakimoto T. 2007. The secretory peptide gene EPF1 enforces the stomatal one-cell-spacing rule. *Genes & Development* **21**: 1720–1725.

Hara K, Yokoo T, Kajita R, Onishi T, Yahata S, Peterson KM, Torii KU, Kakimoto T. 2009. Epidermal cell density is autoregulated via a secretory peptide, EPIDERMAL PATTERNING FACTOR 2 in *Arabidopsis* leaves. *Plant and Cell Physiology* **50**: 1019–1031.

Hunt L, Bailey KJ, Gray JE. 2010. The signalling peptide EPFL9 is a positive regulator of stomatal development. *New Phytologist* **186**: 609–614.

Hunt L, Gray JE. 2009. The signaling peptide EPF2 controls asymmetric cell divisions during stomatal development. *Current Biology* **19**: 864–869.

Lammertsma EI, de Boer HJ, Dekker SC, Dilcher DL, Lotter AF, Wagner-Cremer F. 2011. Global CO_2 rise leads to reduced maximum stomatal conductance in Florida vegetation. *Proceedings of the National Academy of Sciences, USA* **108**: 4035–4040.

Lampard GR, MacAlister CA, Bergmann DC. 2008. *Arabidopsis* stomatal initiation is controlled by MAPK-mediated regulation of the bHLH SPEECHLESS. *Science* **322**: 1113–1116.

Lau OS, Bergmann DC. 2012. Stomatal development: a plant's perspective on cell polarity, cell fate transitions and intercellular communication. *Development* **139**: 3683–3692.

Lawson T, Blatt MR. 2014. Stomatal size, speed, and responsiveness impact on photosynthesis and water use efficiency. *Plant Physiology* **164**: 1556–1570.

Leakey ADB, Ainsworth EA, Bernacchi CJ, Rogers A, Long SP, Ort DR. 2009. Elevated CO_2 effects on plant carbon, nitrogen, and water relations: six important lessons from FACE. *Journal of Experimental Botany* **60**: 2859–2876.

Lee JS, Hnilova M, Maes M, Lin Y-CL, Putarjunan A, Han S-K, Avila J, Torii KU. 2015. Competitive binding of antagonistic peptides fine-tunes stomatal patterning. *Nature* **522**: 439–443.

Lee JS, Kuroha T, Hnilova M, Khatayevich D, Kanaoka MM, McAbee JM, Sarikaya M, Tamerler C, Torii KU. 2012. Direct interaction of ligand-receptor pairs specifying stomatal patterning. *Genes & Development* **26**: 126–136.

Masle J, Gilmore SR, Farquhar GD. 2005. The ERECTA gene regulates plant transpiration efficiency in *Arabidopsis*. *Nature* **436**: 866–870.

Nadeau JA, Sack FD. 2002. Control of stomatal distribution on the *Arabidopsis* leaf surface. *Science* **296**: 1697–1700.

Nobel PS, Zaragoza LJ, Smith WK. 1975. Relation between mesophyll surface area, photosynthetic rate, and illumination level during development for leaves of *Plectranthus parviflorus* Henckel. *Plant Physiology* **55**: 1067–1070.

Pillitteri LJ, Torii KU. 2012. Mechanisms of stomatal development. *Annual Review of Plant Biology* **63**: 591–614.

Qi X, Han S-K, Dang JH, Garrick JM, Ito M, Hofstetter AK, Torii KU. 2017. Autocrine regulation of stomatal differentiation potential by EPF1 and ERECTA-LIKE1 ligand-receptor signaling. *eLife* **6**: e24102.

Seibt U, Rajabi A, Griffiths H, Berry JA. 2008. Carbon isotopes and water use efficiency: sense and sensitivity. *Oecologia* **155**: 441–454.

Shpak ED, McAbee JM, Pillitteri LJ, Torii KU. 2005. Stomatal patterning and differentiation by synergistic interactions of receptor kinases. *Science* **309**: 290–293.

Sugano S, Shimada T, Imai Y, Okawa K, Tamai A, Mori M, Hara-Nishimura I. 2009. Stomagen positively regulates stomatal density in *Arabidopsis*. *Nature* **463**: 241–244.

Tanaka Y, Sugano SS, Shimada T, Hara-Nishimura I. 2013. Enhancement of leaf photosynthetic capacity through increased stomatal density in *Arabidopsis*. *New Phytologist* **198**: 757–764.

Terashima I, Hanba YT, Tazoe Y, Vyas P, Yano S. 2006. Irradiance and phenotype: comparative eco-development of sun and shade leaves in relation to photosynthetic CO_2 diffusion. *Journal of Experimental Botany* **57**: 343–354.

Terashima I, Hanba YT, Tholen D, Niinemets U. 2011. Leaf functional anatomy in relation to photosynthesis. *Plant Physiology* **155**: 108–116.

Torii KU, Mitsukawa N, Oosumi T, Matsuura Y, Yokoyama R, Whittier RF, Komeda Y. 1996. The *Arabidopsis* ERECTA gene encodes a putative receptor protein kinase with extracellular leucine-rich repeats. *Plant Cell* **8**: 735–746.

Wuyts N, Palauqui JC, Conejero G, Verdeil JL, Granier C, Massonnet C. 2010. High-contrast three-dimensional imaging of the *Arabidopsis* leaf enables the analysis of cell dimensions in the epidermis and mesophyll. *Plant Methods* **6**: 17.

Supporting Information

Additional Supporting Information may be found online in the Supporting Information tab for this article:

Table S1 Summary of gas-exchange (g_{smax}) and photosynthetic (V_{cmax}) capacity among stomatal development mutants and the impact on water-use efficiency ($\delta^{13}C$)

Table S2 Summary of cell anatomical features and leaf attributes for all controls and genotypes visualized using three-dimensional confocal microscopy

Table S3 Test of epistasis among signaling genotypes and double mutants using stomatal density (SD) to palisade mesophyll density (PMD) ratio

Please note: Wiley Blackwell are not responsible for the content or functionality of any Supporting Information supplied by the authors. Any queries (other than missing material) should be directed to the *New Phytologist* Central Office.